High Gain Frequency Domain Optical Parametric Amplification

Philippe Lassonde, Nicolas Thiré, Ladan Arissian, Guilmot Ernotte, François Poitras, Tsuneyuki Ozaki, Antoine Lorameé, Maxime Boivin, Heide Ibrahim, François Légaré, and Bruno E. Schmidt

(Invited Paper)

***Abstract*—The powerful technique of optical parametric amplification (OPA) experienced a huge advance with the invention of optical parametric chirped pulse amplification (OPCPA) and later noncollinear OPA. In this paper, we describe a radically different approach of performing parametric interaction in the frequency domain instead of the time domain. The frequency domain is reached via optical Fourier transformation, which provides a separation ansatz. It allows breaking down a big task into smaller ones which ultimately enables simultaneous up-scaling of peak power and bandwidth. The first proof-of-concept experiment yielding 1.4 mJ, two cycle pulses at 1.8-μm wavelength is complemented by a high gain (>2000) setup at 800-nm wavelength with 2.5 kHz repetition rate. A very low amount of parasitic superfluorescence without degradation of the picosecond pulse contrast within the pump pulse duration has been observed upon high gain conditions.**

***Index Terms*—Nonlinear optics, optical parametric amplification, few-cycle pulses.**

I. Introduction

DURING the first decade after its birth in 2001 [1], [2], attosecond science was probably one of the biggest beneficiaries of the steadily improving high energy femtosecond laser technology [3]. The second decade was then heralded by the demand of attosecond science for new pulse parameters like the tailoring of the electric field rather than just its intensity envelope [4] and thus pushing laser science forward. Thereupon different schemes have been proposed [5]–[7] which all have in common that their required spectral bandwidths outreach by far the gain bandwidth of established Ti:Sa amplifiers.

By contrast with these real level gain media based on population inversion, the bandwidth of parametric processes involving virtual levels is not constrained by a limited band of electronic or vibrational transitions. Although the gain bandwidth of OPA is only limited by linear as well as nonlinear absorption of the three interacting light fields (pump, signal and idler), a number of restrictions hamper its full exploitation.

The most vigorous one arises from the fact that efficient energy transfer from pump (*p*) to signal (*s*) and idler (*i*) waves requires the conservation of energy ($\hbar\omega_p = \hbar\omega_s + \hbar\omega_i$) and momentum ($\vec{k}_p = \vec{k}_s + \vec{k}_i$) between interacting waves. The latter, generally referred to as phase matching condition[1] cannot be satisfied in a dispersive medium and birefringent materials are typically utilized to adjust for different light velocities.

In this paper, new design opportunities and challenges arising from parametric amplification in the frequency domain [8] are presented and discussed in comparison with OPCPA. Reviewing the principles of OPCPA lies outside the scope of this paper and the reader is referred to other comprehensive reviews [9]–[11].

The principles and characteristic features of frequency domain optical parametric amplification (FOPA) are explained in Section II. Experimental results on how dispersion limitations as well as peak power scaling can be overcome are presented in Section III followed by results on high gain amplification of nanojoule seed pulses to the microjoule level in Section IV. A detailed discussion of the presented results and future prospects is given in Section V.

II. FOPA Principles

The essential idea of FOPA is illustrated in Fig. 1 which shows a symmetric *4f* setup. The colours of a collimated input pulse ($\Delta\lambda_{\mathrm{pulse}}$) are dispersed on the first grating G1 and become parallel behind the collimating mirror M1 if placed at the focal distance *f* from the grating. Each of the reflected colours is focused into its separate focus ($\Delta\lambda_{\mathrm{foc}}$) and all foci line up next to each other in the Fourier plane (FP). Until here a first (continuous) optical Fourier transformation from the time domain into the frequency domain has been performed at the speed of light. It will become important later that each point of the beam profile outside the 4*f* setup contains all spectral components ($\Delta\lambda_{\mathrm{pulse}}$) whereas in each focal point at the FP the spectral variation ($\Delta\lambda_{\mathrm{foc}}$) is orders of magnitude smaller. A symmetric setup on

Manuscript received December 23, 2014; revised February 20, 2015, March 24, 2015, and March 25, 2015; accepted March 25, 2015. This work was supported in part by NSERC, CIPI, FRQNT, MDEIE, and the DARPA PULSE program under a grant from AMRDEC.

P. Lassonde, N. Thiré, G. Ernotte, F. Poitras, T. Ozaki, A. Lorameé, M. Boivin, H. Ibrahim, and F. Légaré are with the Centre ÉMT, Institut National de la Recherche Scientifique, Varennes, QC J3X1S2, Canada (e-mail: lassonde@emt.inrs.ca; thire@emt.inrs.ca; guilmot.ernotte@emt.inrs.ca; poitras@emt.inrs.ca; ozaki@emt.inrs.ca; laramee@emt.inrs.ca; boivin@emt.inrs.ca; ibrahim@emt.inrs.ca; legare@emt.inrs.ca).

L. Arissian is with the Department of Electrical and Computer Engineering, University of New Mexico, Albuquerque, NM 87106 USA (e-mail: aladan@uottawa.ca).

B. E. Schmidt is with the Centre ÉMT, Institut National de la Recherche Scientifique, Varennes, QC J3X1S2, Canada, and also with few-cycle Inc., Montréal, QC H1L5W5, Canada (e-mail: schmidt@few-cycle.com).

Color versions of one or more of the figures in this paper are available online at http://ieeexplore.ieee.org.

Digital Object Identifier 10.1109/JSTQE.2015.2418293

[1]Phase matching is necessary for a coherent growth of signal and idler waves which requires the propagating light waves to stay in phase with the induced nonlinear polarization waves over the entire propagation length. The connection between light and polarization waves is the (nonlinear) susceptibility.

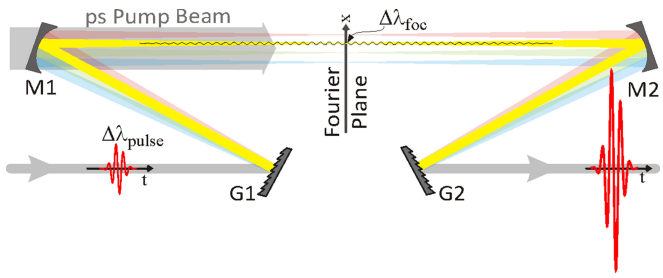

Fig. 1. The FOPA setup rests upon a *4f* configuration which maps the spectral content of an incident few-cycle pulse onto a spatial coordinate in the FP. There, the seed beam is intrinsically stretched to picosecond duration (see Fig. 2) and can interact with a picosecond pump beam. A separate stretcher or compressor, respectively, is not required. Different, individually tunable crystals may be employed in the FP. Thus, by increasing the number of crystals, the FOPA output properties like energy or bandwidth are not limited by the performance of a single crystal.

the other side of the FP performs a second Fourier transformation and recovers the original beam in time domain. Such an arrangement in combination with mode locked lasers was first introduced in 1981 for picosecond pulse shaping purposes [12]. Pulse shaping is generally achieved through attenuation of spectral amplitudes in the FP and by shifting their relative phases. In this sense, FOPA is a pulse shaping unit which now allows one to additionally introduce a gain element in the FP. In contrast, established femtosecond laser amplification techniques, either CPA or OPCPA, are based on interaction of pump and seed pulses in time domain. The detour of performing amplification in between two Fourier transformations in FOPA seems like an additional constrain at first sight. On the other hand, all OPCPA's necessarily require pulse stretching and compression schemes which become obsolete with FOPA. It can be seeded with transform limited as well as arbitrarily shaped pulses. Although challenging, pulse shaping of octave spanning spectra has been demonstrated with *4f* setups [13], [14]. Small translations of the second exit grating G2 can be used to compensate modest chirp introduced by amplification crystals or optical windows. Unlike with usual grating compressors, positive and negative chirp can be set. This option becomes relevant in the IR region where many glasses exhibit zero dispersion and thus, by changing the transmission optics one might have to switch from negative to positive chirp.

Once the challenge of designing an appropriate *4f* setup is mastered a number of new design opportunities arise which are hardly achievable in time domain schemes. One of the most important aspects of optical Fourier transformation according to Fig. 1 is the mapping of spectral frequencies onto a spatial coordinate in the FP. Each frequency is focused onto its corresponding point in the FP and the entire spectrum spreads out along a line focus. It literally gives direct access to the pulse's properties, i.e., its frequency components. This spatial branching can be viewed as a separation ansatz allowing the breakdown of a big task and accomplishing it by solving several smaller ones.

Such a big task is for instance ultrabroadband phase-matching which is a major concern in OPA. If for a given combination of crystal and interacting light fields the phase mismatch approaches π, the task may be solved by distributing the same bandwidth over more than one crystal. With two or more crystals being placed next to each other in the FP each one has to amplify a much narrower bandwidth. Independent tuning of different crystals in sum enables a much broader phase-matching bandwidth than would be possible with a single crystal of the same length. Other schemes like non-collinear phase-matching can be applied as well [15]–[19]. In principle, differently grown crystals or even different materials could be combined as long as the optical path remains the same for all spectral components. One way to equalize optical path lengths could be the insertion of tunable glass plates of the same size in front of each crystal to build a simplified phase shaper.

Another big task to be resolved is the crystals' damage threshold. The only way to circumvent this is to increase the incident beam size which, however, is ultimately limited by the maximum available crystal size [19]. FOPA resolves this problem by enabling the use a mosaic of crystals to increase the total size of the gain medium without affecting the spatial beam quality. Therefore one merely needs to further spread out the spectrum in the FP by using a more dispersive grating. In standard schemes, increasing the parametric gain through longer crystals increases the phase mismatch and thus reduces the bandwidth. In FOPA, this can be circumvented by keeping the same spread along the FP but using several crystals with smaller aperture such that each one receives a smaller incident bandwidth.

As a result, the output properties of FOPA are not limited by the performance of a single crystal anymore. Achieving a desired performance becomes a matter of the number of crystals employed and less of the crystal itself. Moreover, increasing phase-matching bandwidth and pulse energy can be achieved simultaneously, a situation that is completely reversed for OPCPAs where fulfilling one of these big tasks typically denotes a trade-off on the other one.

Having an even closer look at the FP reveals further advantages compared to OPCPA. In each focal point, the spectral variation across the focus ($\Delta\lambda_{\mathrm{foc}}$) is very small. Its amount is a function of grating dispersion and input beam diameter but it is, however, independent of the focal length of M1 and M2, respectively. As an example, for the more challenging design case of octave spanning spectra the typical bandwidth across the focus is about 300–600 times less than the total pulse bandwidth. This means, a single cycle input pulse will be automatically stretched to picosecond duration in the FP. The duration depends on the geometrical properties like the grating groove separation g and the input beam size d_{in} at FWHM. The pulse duration at FWHM of intensity is given by:

$$\Delta t_{\mathrm{foc}} = \frac{\lambda_c d_{\mathrm{in}}}{gc}\left[1-\left(\frac{\lambda_c}{2g}\right)^2\right]^{-1/2} \tag{1}$$

with λ_c being the center wavelength and c the speed of light. The derivation of (1) is shown in the appendix. It is pointed out that the pulse duration in the FP is independent of the focal length f and the input pulse bandwidth $\Delta\lambda_{\mathrm{pulse}}$. Moreover, since the spectrum in each focal point is reduced by 2–3 orders of magnitude it can be viewed as a quasi-monochromatic

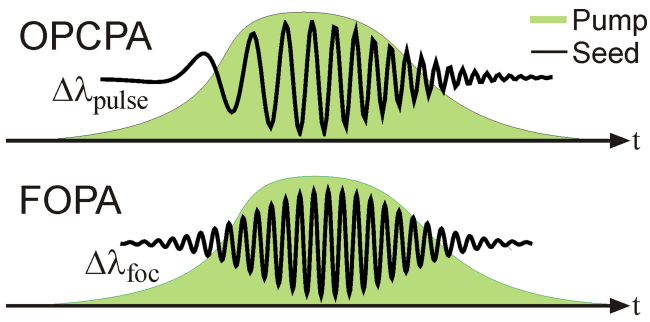

Fig. 2. Comparison between OPCPA and FOPA. Time domain schemes (OPCPA) rely on temporal chirping with the result that each wavelength experiences a different gain. In frequency domain schemes (FOPA), however, only a small fraction of the entire pulse bandwidth $\Delta\lambda_{\mathrm{pulse}}$ is present in each focal point $\Delta\lambda_{\mathrm{foc}}$ in the FP. The pump pulse envelope has minor influence on the spectrum of this quasi-monochromatic beam. Furthermore, the intensity in each focal point can be tailored, see Fig. 3.

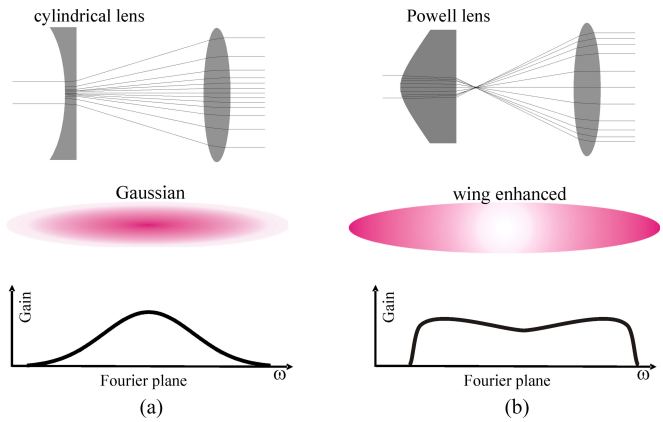

Fig. 3. The intensity distribution in the FP defines the spectral gain curve. While beam expansion of Gaussian distributions with spherical cylindrical lenses still leads to Gaussian distributions along the FP, special aspheric telescopes or free form surfaces could be used to tailor the gain function arbitrarily.

beam. In contrast, all time domain schemes deliver broadband strongly chirped seed pulses carrying the entire pulse bandwidth ($\Delta\lambda_{\mathrm{pulse}}$) in the interaction region. This imposes additional constraints regarding the matching of pump pulse duration and desired gain bandwidth. Even if the phase-matched bandwidth covers the desired range, the gain bandwidth can be limited by too short pump pulse durations as illustrated qualitatively in Fig. 2. In the case of OPCPA, matching the FWHM of pump with the one of the seed pulse to reach the highest efficiency might reduce the gain bandwidth simply because the pump intensity is lower in pulse tails. This causes a reduction of amplified bandwidth as depicted in Fig. 2. Thus, there is a trade-off between highest gain and broadest bandwidth and different pump pulse shaping strategies have been proposed for its minimization [20]. Owing to the separation ansatz of FOPA, the situation is different in the FP. When matching the envelopes of the pump with a quasi-monochromatic seed in each focal point, varying the pump pulse duration doesn't reduce the amplified bandwidth $\Delta\lambda_{\mathrm{foc}}$ in this point and hence does not reduce the total pulse bandwidth at the output. $\Delta\lambda_{\mathrm{foc}}$ defines the pulse duration and thus the seed intensity in the FP. In conventional time domain schemes the seed intensity quadratically depends on the input beam diameter. In FOPA, changing the seed beam input diameter d_{in} automatically changes both the focus area ($\sim d_{\mathrm{in}}^2$) and the pulse duration ($\sim d_{\mathrm{in}}$) by changing $\Delta\lambda_{\mathrm{foc}}$. Thus, the seed intensity in the FP depends linearly on the input beam diameter.

Coming back to Fig. 1, we emphasize that additionally to the temporal Fourier transformation, a *4f* setup with spherical optics also provides a spatial Fourier transformation by focusing a collimated input beam into a focal spot in the FP. This means, parametric interaction with the pump beam takes place with a spatially (and temporally) Fourier transformed beam. Consequently, spatial impurities like hot spots present in the pump beam are not transferred to the amplified beam after its second spatial Fourier transformation subsequent to amplification.

These explanations of conditions and design opportunities regarding the seed beam are followed by a description of the design opportunities for the pump beam. Due to the spatial separation of frequency components, FOPA is especially attractive for multi-beam pumping schemes. Single frequency pump beams incident at different angles [21] or multi-colour beams where different spectral parts get amplified by different pump wavelengths [22]–[24] could be applied.

Even in the case of a single pump beam far-reaching design opportunities arise through spatial shaping of the pump intensity. Because of the intensity dependent parametric gain [23], [24] the gain function can be arbitrarily modified by an appropriate intensity distribution. Apart from adaptive beam shaping methods, one could also employ freeform optics or aspherical optics. Beam expansion with cylindrical optics does not change the shape but rather the slope of the intensity distribution and a Gaussian beam would thus still lead to a Gaussian intensity (gain) profile along the FP as shown in Fig. 3(a). Beam expansion with a special asphere, the so called Powell lens [26], is depicted in Fig. 3(b) for comparison. Its main function is to further spread out the rays in the wings of the beam than at its centre. This lens typically consists of an aspheric and a plane surface. Subsequent to the one-dimensional aspheric surface all beams intersect in a single line similar to a conventional focusing optic and the beam can be collimated with a cylindrical lens. The exact intensity distribution subsequent to the collimating lens depends on the input beam diameter and the distance between the two lenses. Such a properly designed flat-top beam shaping telescope does not cause additional losses since it requires the same amount of optics (two) as a conventional one would. In this manner, flat-top or wing enhanced intensity distributions can be achieved in a robust way and the gain function can be tailored to boost the wings of a spectral distribution as shown in Fig. 3(b).

III. High Energy FOPA

This section briefly summarizes the proof of concept FOPA experiment [8] together with an additional characterization of the output beam properties. The experiment aimed at generating the highest energy 2-cycle IR pulses at 1.8 μm. These results

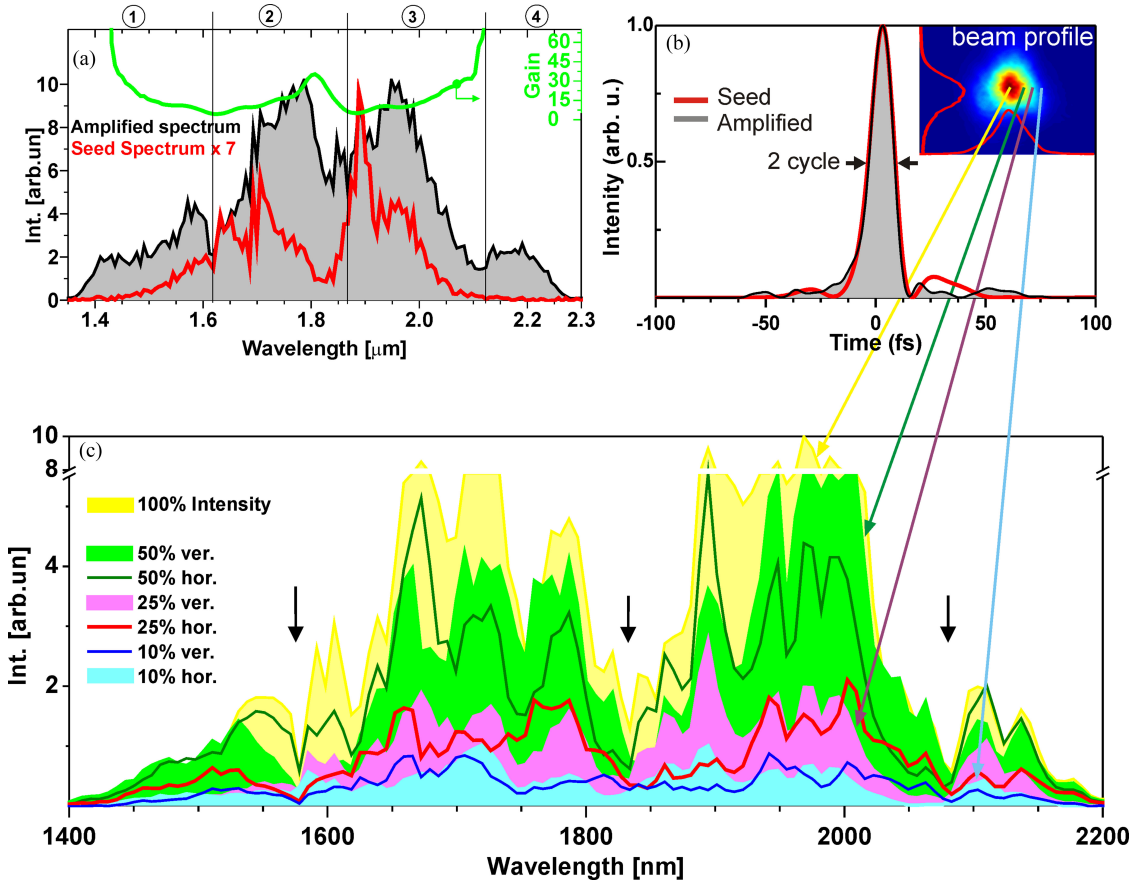

Fig. 4. Results of high energy FOPA yielding two cycle pulses with 1.43 mJ pulse energy. (a) Comparison of seed (red) and amplified (shaded grey) spectra. The vertical lines indicate the spectral ranges for each of the four crystals in the FP. The spectral shape is preserved with a noticeable increase towards the wings of the spectrum. The gain function (green) was tailored with an aspheric telescope as described in Fig. 3(b). (b) Temporal intensity profiles for seed (red) and amplified beam (grey) retrieved from SHG-FROG measurements. The spatial beam profile is shown in the inset. (c) Absence of spectral chirp across the spatial beam profile subsequent to the FOPA. The curves show the spectra at different positions in the beam as explained in the legend, note the broken ordinate.

on high energy amplification (gain of 14) are complemented in a second experiment described in Section IV. This FOPA was realized at a high repetition rate of 2.5 kHz and as a high gain stage with 2000 times amplification from nanojoule to the microjoule level. Such conditions are typical in primary amplification stages to amplify an oscillator output for instance.

The first, high energy FOPA was realized on the 100 Hz, carrier to envelope phase (CEP) stable, sub-2 cycle IR beam line at the Advanced Laser Light Source [27] and is described in detail in Ref. [8]. 800 nm pulses from a Ti:Sa amplifier are used to drive the parametric amplification. The FOPA design employed four BBO crystals in the FP to amplify a narrow bandwidth from 1.35 to 2.25 μm, shown as magnified red curve in Fig. 4(a). The spectral range incident on each crystal (1)–(4) is marked by vertical lines. The jagged appearance of the curves is due to the poor signal to noise ratio (S/N) of the spectrometer.

While under the given conditions (cut of BBO crystal, pump and seed wavelengths) less than four crystals could be sufficient to phase-match the entire bandwidth, we aimed to prove the scaling capability and to verify whether detrimental effects occur from a multi crystal arrangement. Since the manufacturing reproducibility of the crystal thickness on a wavelength scale is hard to achieve, all four crystals were polished together (United Crystals). The absolute thickness is only known with sub 50 μm precision but the relative deviation is kept below the wavelength range. The crystals, when placed side by side, would cover 60 mm in the FP. Each frequency of the seed pulse is focused to a spot size of about 220 μm at FWHM of intensity. This, in combination with the grating dispersion corresponds to a pulse duration of 1.4 ps. The pump beam was expanded with a Powell lens telescope as shown in Fig. 3(b) to achieve a tailored intensity distribution along the FP with a 5–10% increase towards the edges. Its temporal duration was optimized for maximum gain. Pump and seed focal spot sizes were measured to be 300 and 220 μm, respectively. The total of 13 mJ pump energy delivered to the entire FP corresponds to an intensity of roughly 40 GW/cm^2. At this pump level the output energy increased from 0.1 to 1.43 mJ denoting a gain of 14 with a pump (1.55 eV) to idler (0.68 eV) conversion efficiency of 14% measured in the FP. The spectrum at maximum gain (black curve in Fig. 4(a)) is overlaid with the input spectrum. It can be seen that the spectral extension remains unchanged upon amplification and even shows an enhancement in the wings, following the pump intensity pattern. This is clearly confirmed by the experimental gain

curve (green). The credibility of its absolute values in the wings is limited due to the poor S/N ratio of the seed.

The temporal shape has been characterized with SHG-FROG [10], [26] and the comparison of seed pulses prior to the FOPA as well as at maximum gain is presented in Fig. 4(b). Remarkably, the shape of the main pulse stays the same and temporal FWHM increases marginally from 11.5 to 11.7fs. At 1.8 μm wavelength 12 fs duration at FWHM of intensity correspond to two cycles of the electric field. Examining the seed (red) and amplified (grey) pulses in Fig. 4(b) reveals no change of the main pulse, only a slightly modified pedestal structure below the 5% level. This mainly stems from the 4*f* setup with the four crystals itself and is not an amplification artefact. An exhaustive discussion about the pedestals can be found in Ref [8].

After confirming excellent spectral and temporal properties the spatial beam quality was investigated. As expected, it is not influenced by the sharp crystal edges in the FP and is shown in the inset of Fig. 4(b). In this regard, we also verified the reduced requirements of a clean pump beam profile. Therefore, a sharp edge was introduced in the pump beam by inserting a beam blocker. This resulted in a homogeneous intensity decrease of the amplified output beam without affecting its shape. Next, the spatial chirp, i.e. the variation of spectrum across the beam profile, was investigated. A 400 μm fibre tip coupled to the IR spectrometer was scanned transversely across the amplified output beam in vertical and horizontal direction with the result plotted in Fig. 4(c). The strong spectral modulations are an artefact of the coupling to a multimode fibre and the dips resulting from crystal edges are marked by black arrows. Unfortunately, the spectral resolution is too low to resolve the actual spectral incisions from the crystal edges. The spectrum at the beam centre is shown as the yellow curve and plotted versus a broken ordinate. Both greenish curves show the spectrum at 50% of intensity along the horizontal and vertical direction, respectively. The same applies to the reddish and bluish curves at 25% and 12% level, respectively. This data clearly confirms the absence of spatial chirp.

The final characterization concerned the CEP stability which was measured with an *f*-2*f* interferometer [29]. The seed pulses were passively stabilized [30] and no feedback loop for additional stabilization was implemented. The CEP stability of the seed pulses was 320 mrad which increased to 460 mrad after amplification [8]. The already low CEP stability of the seed pulses may result from issues with the hollow-core fibre compression [31] and might relate to the observed pointing fluctuations after the fibre. Nevertheless, the conclusion from this first experiment is that FOPA supports CEP stable amplification of two cycle pulses from 100 μJ to 1.4 mJ without the need for a pulse shaping device and without degradation of spatial or temporal pulse quality. This experiment confirmed the capability of FOPA for being utilized as a booster in a high energy stage.

IV. High Gain FOPA

In the second experiment a setup for high amplification gain at lower energy is described which aims to address two aspects of using FOPA as a robust amplifier module. First, FOPA has to be capable of serving as a front end of an amplifier chain. Second, the picosecond contrast should be maintained over a wide range of gain. The latter is crucial in high energy physics experiments [32]–[35]. Since the aspects of wavelength conversion and few-cycle operation have been addressed previously using IR pulses, we were satisfied with the typical Ti:Sa performance for the second experiment and the high gain FOPA was built with standard stock items. The experimental setup is shown in Fig. 5.

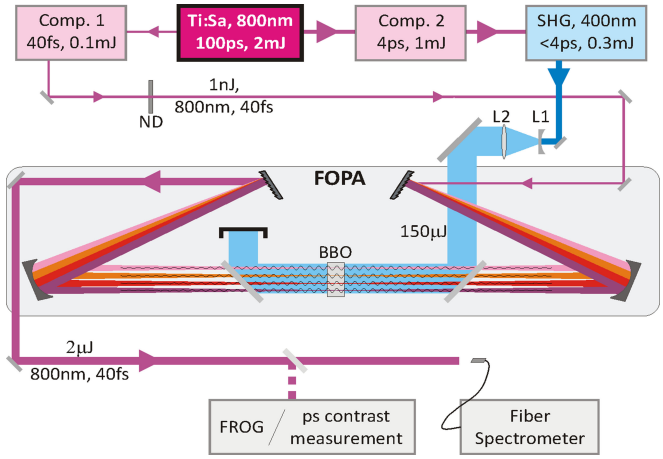

Fig. 5. Setup for high gain FOPA at 2.5 kHz repetition rate. Nanojoule level seed pulses at 800 nm (purple line) are amplified 2000 times with a 2 mm thick BBO crystal in the FP pumped by ~3 ps frequency doubled pulses (blue line).

The starting point is a 2.5 kHz Ti:Sa CPA which delivers 2 mJ pulse energy before compression. A small fraction was compressed to 40 fs with 100 μJ energy. The energy was further reduced with neutral density filters down to the nanojoule level which represents typical starting conditions for an amplifier chain. These pulses were used to seed a FOPA and were subsequently launched to different diagnostics. A fibre spectrometer served to verify the absence of spatial chirp and a transient grating-frequency resolved optical gating (TG-FROG) setup [28] was used to characterize both the pulse duration and the picosecond pulse contrast. Since we aimed for investigating the picosecond contrast, only a single BBO crystal ($\Theta = 29°$) of 2 mm thickness was placed in the FP. The reason to use a single crystal was to avoid sharp edges in the FP. Simulations showed that sharp spectral dips may result in reduced picosecond contrast on the level of 10^6 [8]. In the present experiment, the interest was to study parametric interaction in the frequency domain as such. We aimed to verify if the presence of picosecond pump and picosecond seed pulses in the FP influences the picosecond pulse contrast of the recompressed output. The FOPA used in the experiment consisted of two silver coated gratings (1200 l/mm), two spherical mirrors ($f = 200$ mm) and two dichroic beam splitters to overlap pump and seed beams close to collinearly for simplicity reasons. The exit grating was mounted on a translation stage to fine tune the dispersion. With a seed input beam diameter of roughly 1 mm FWHM of intensity the calculated duration in the FP amounts to 3.6 ps according to Eq. (1).

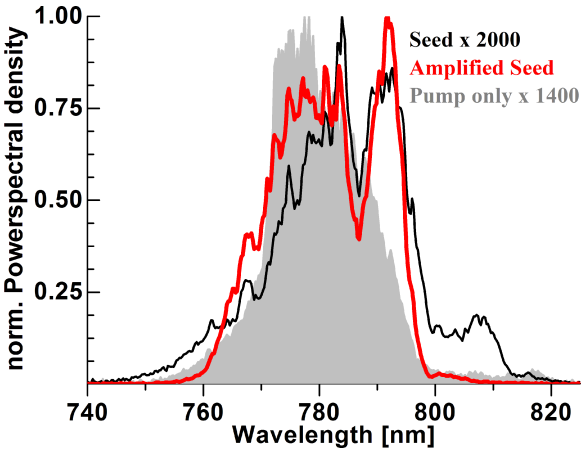

Fig. 6. Experimental spectra of seed (black) and amplified beam (red) obtained with the setup shown in Fig. 5. Like in Fig. 4(c), the spectral shape remains the same apart from lower gain in the wings because we did not use a special telescope to tailor the gain function as explained in Fig. 3(b). The grey curve shows the spectrum of superfluorescence in the unseeded case.

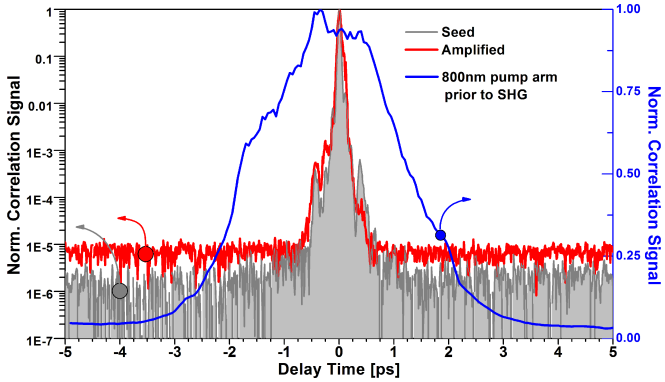

Fig. 7. Third order correlation signals obtained from transient grating optical gating. The 800 nm pump pulse prior to doubling is shown in blue on a linear scale. The contrast within the pump window at ± 1 ps is not affected at 2000 fold amplification.

To provide the pump beam, the majority of the 800 nm Ti:Sa laser was compressed to less than 4 ps duration to match the seed duration in the FP. The beam was frequency doubled with 30% efficiency in a 1 mm thick BBO crystal. Including optical losses of silver mirrors and uncoated lenses the maximum pump energy delivered to the FP was 150 μJ. For convenience, only spherical cylindrical lenses were employed to provide a Gaussian pump intensity distribution in the FP.

The amplified spectrum after a 2000 fold increase is shown in Fig. 6 as the red curve and is overlaid with the seed spectrum in black whose output energy was raised from 1 nJ to 2 μJ. Since no gain tailoring telescope was used in this experiment, a slight loss of bandwidth in the wings becomes visible while the FWHM and the overall shape remains the same, like in the first experiment. It is noteworthy that all spectral features like the dip at 790 nm and the small plateau above 800 nm are transferred despite the high gain. To achieve the highest gain, the grating compressor of the Ti:Sa laser was tuned from 2.5 to 5 ps. A change of the output spectral shape was not observed but merely a homogeneous increase and decrease.

As a first step to quantify the generated amount of parasitic superfluorescence the seed beam was blocked and the output spectrum was measured in otherwise identical conditions, see the shaded grey curve in Fig. 6. As expected, its bandwidth is similar to the amplified one since it is determined by the phase matching conditions of the parametric interaction [36], [37]. A low superfluorescence level of 7×10^{-4} was measured for this unseeded collinear parametric amplifier. Comparable values are reported for non-collinear interaction which intrinsically provide less background [38]. Finally, the picosecond contrast was characterized with a home built TG-FROG. This arrangement was chosen because it allows to characterize the electric field and the picosecond contrast since it is a background free method. Building a TG-FROG was necessary because the commercial devices (Sequoia, Amplitude technologies) cannot be operated with our low input energy of 1 μJ. The commercial device, however, was used to confirm the measurement of the home built device. Since the TG-FROG employs a third order nonlinearity for optical gating it allows direct measurement of asymmetric pulse shapes like the third harmonic correlation technique [39]. First, the optimized 800 nm pump pulse was characterized and is given as the blue curve in Fig. 7 on a linear scale. Its deconvolved FWHM duration is about 3 ps. The duration of the second harmonic has not been measured but is expected to be similar or even slightly shorter. All presented correlation traces are obtained from integrating the 2-D spectrogram with respect to the frequency axis. Next, the contrast of the seed pulse was measured before and after the FOPA without amplification to ensure that no distortion is introduced by the *4f* setup. The seed pulse prior to the FOPA was also characterized with the commercial device and yielded good agreement with our method. Using the commercial device in this situation was possible because the input energy could be raised to 100 μJ by removing the attenuation filters. The drawback of our home built setup was the lower dynamic range when operated with 1 μJ pulse energy incident on the nonlinear medium (2 mm FS). The grey curve in Fig. 7 shows the seed contrast as a semi logarithmic plot. The dynamic range is limited to 10^6. However, evaluating the contrast outside the pump pulse duration (below -3 ps and above $+3$ ps) is not relevant because it cannot be amplified there in the parametric process. Within the pump window from -2 to 1.5 ps all pedestals can be detected. As can be seen at ± 1 ps, the seed contrast of the input pulses is about 10^5. The red curve shows the correlation for the 2 μJ pulses after a 2000 fold amplification. The temporal FWHM duration increased from 38 to 41 fs (not resolved in Fig. 7). The dynamic range was lowered to 10^5 because less energy was available compared to the seed case without attenuation filter. Nevertheless, the most important part at ± 1 ps can still be analyzed. Although at the detection limit it can be seen that the contrast there is at least 10^5 which is identical to the one of the seed beam. The conclusion is that the picosecond contrast has not changed within the pump window after a 2000 fold amplification.

V. Discussion

The first high energy experiment utilizing the multi crystal FOPA setup described in Section III confirmed the modular nature of the FOPA concept. It proved that its output properties

like energy and bandwidth are defined by the sum of individual components, each of them being individually optimized. While in this experiment only the phase matching angle was optimized, other parameters like type of crystal, the crystal shape, the pump wavelength and intensity may be optimized in the future.

So far, FOPA's only conceptual drawback identified is the potential reduction of picosecond pulse contrast originating from the sharp spectral incisions when multiple crystals are used. Simulations have shown that the contrast increases by reducing the number of incisions, their width or their edge sharpness. The latter two may be minimized by ensuring a focal spot size larger than the crystal gap. In that case when every colour gets smeared out across the gap sharp edges in the spectrum are avoided. By this, the picosecond contrast can be improved by orders of magnitude. Before investigating the influence of multiple crystal gaps on the picosecond contrast we generally confirmed that a picosecond contrast degradation as such is not to be expected from the picosecond interaction in the FP.

Furthermore, it was shown that FOPA can be implemented as a high gain stage for nanojoule level seed pulses at high repetition rates. The 2 μJ output is less than the expected $\sim$10 μJ and can be explained by: (i) the fact that the Gaussian pump focus had to exceed the spectral extension to provide sufficient amplification in the spectral wings; (ii) we noticed severe focal distortions if the average power in the grating compressor exceeded 3 W which further reduced the pump intensity. In this regard it is mentioned that by decreasing the focal extension along the FP to amplify a narrow bandwidth of only 10 nm a gain of 12 000 was measured.

It is pointed out that all design considerations for building an OPCPA can be directly applied to FOPA in a single crystal configuration as well. Even in that configuration, FOPA still provides advantages compared to OPCPA. Neither stretcher nor compressor are required to amplify two cycle pulses to the microjoule level and fine tuning of small amounts of chirp can be achieved with the exit grating. Straightforward tailoring of the gain curve by shaping the spatial pump beam intensity distribution can be achieved with lens telescopes instead of shaping the temporal pump shape as was proposed for OPCPA [20], [40]. Furthermore, the quasi-monochromatic seed beams present in the FP allow for maximizing extraction efficiency by optimizing the pump pulse duration without influencing the spectral bandwidth.

After the discussion of new design opportunities we like to turn to the challenges.

One concern could be the use of beam splitters for combining pump and seed beams in the vicinity of the FP plane which have to support high intensities and a large bandwidth. Octave spanning operation is straight forward if the broadband pulse is to be transmitted and only the narrowband pump pulse needs to be reflected. If, however, an appropriate beam splitter is not available, a non-collinear configuration can be chosen without affecting the amplified beam quality.

A real bottleneck is the availability of suitable diffraction gratings. The exit grating is the first surface in the FOPA where all the bandwidth and amplified power is recombined to a single beam. The demands on the grating are high efficiency over wide bandwidth, high damage threshold and good resistance to high average power. Brewster prisms would solve the spectral efficiency problem but would fail at high average and peak powers, respectively. Gratings that support two cycle pulses can be found in various spectral ranges, however, good efficiencies for octave exceeding bandwidths might be easier obtained in the IR than in the VIS region. In the IR range a two octave spanning FOPA seems feasible. The threshold for peak power damage needs to be undercut by providing the proper beam size and at high average powers water cooled copper gratings could become the right choice.

In summary, FOPA has been introduced as a new concept in which the laser output parameters are not restricted by the performance of a single crystal anymore. Simultaneous up-scaling of bandwidth and energy becomes a matter of the number of crystals employed. This scaling principle was confirmed experimentally by employing four crystals in the FP to achieve sub-2 cycle pulses carrying 1.4 mJ of energy. No detrimental effects either on the spatial beam profile or the temporal profile and femtosecond contrast were observed. With adjacent experiments we demonstrated FOPA's capability as a high gain (2000 and 12 000) device using a 2 mm thick BBO crystal. A single crystal high gain FOPA showed no deterioration of picosecond pulse contrast within the pump pulse duration. The combination of both experiments affirms our goal of building entire laser amplification chains based on FOPA with synchronized high power Ytterbium pump lasers.

APPENDIX

This section is dedicated to the derivation of an analytical expression for the pulse duration Δt_{foc} at FWHM of intensity in the FP. To estimate the pulse duration one needs to evaluate the corresponding spectral content $\Delta\lambda_{\mathrm{foc}}$. We start from the basic grating equation with g being the grating groove separation, m the diffraction order, α and β the incident and diffracted angles, respectively:

$$m\lambda = g\left(\sin\left(\alpha\right) + \sin\left(\beta\right)\right). \tag{A1}$$

For the central wavelength λ_c in first diffraction order ($m = 1$) under Littrow condition ($\alpha = \beta$) we get:

$$\alpha = \operatorname{asin}\left(\frac{\lambda_c}{2g}\right) = \beta_c. \tag{A2}$$

For any other wavelength, the incident angle α remains unchanged and the diffracted angles become:

$$\beta = \operatorname{asin}\left(\frac{\lambda}{g} - \frac{\lambda_c}{2g}\right). \tag{A3}$$

After travelling a distance equal to the focal length f the spatial separation x of wavelengths perpendicular to the propagation direction becomes:

$$\begin{aligned} x &= f\tan\left(\beta - \beta_c\right) \\ &= f\tan\left(\arcsin\left(\frac{\lambda}{g} - \frac{\lambda_c}{2g}\right) - \arcsin\left(\frac{\lambda_c}{2g}\right)\right) \end{aligned} \tag{A4}$$

and with

$$\frac{dx}{d\lambda} = \frac{f}{g}\sec^2\left(\arcsin\left(\frac{\lambda}{g}-\frac{\lambda_c}{2g}\right)-\arcsin\left(\frac{\lambda_c}{2g}\right)\right)\left[\sqrt{1-\left(\frac{\lambda}{g}-\frac{\lambda_c}{2g}\right)^2}\right]^{-1} \quad \text{(A5)}$$

the distribution of wavelengths $\Delta\lambda$ writes as:

$$\Delta\lambda = \frac{\Delta x g}{2f}\sqrt{1-\left(\frac{\lambda}{g}-\frac{\lambda_c}{2g}\right)^2}\left[\cos\left(2\arcsin\left(\frac{\lambda}{g}-\frac{\lambda_c}{2g}\right)-2\arcsin\left(\frac{\lambda_c}{2g}\right)\right)+1\right]. \quad \text{(A6)}$$

If we consider only the distribution for a small wavelength range around the center wavelength $\left(\lim_{\lambda\to\lambda_c} f(\lambda)\right)$, (A6) reduces to:

$$\Delta\lambda_c = \frac{\Delta x g}{f}\sqrt{1-\left(\frac{\lambda_c}{2g}\right)^2}. \quad \text{(A7)}$$

This wavelength distribution can be related to a temporal pulse width by assuming a Gaussian envelope shape:

$$\Delta t = \frac{4\ln(2)}{\Delta\omega} \text{ with } \Delta\omega = \frac{2\pi c}{\lambda^2}\Delta\lambda \quad \text{(A8)}$$

where c denotes the speed of light. Assuming Gaussian beam optics, and by setting the spatial separation Δx equal to the focal spot diameter Δx_{foc} at FWHM of intensity which is given by

$$\Delta x_{\mathrm{foc}} = \frac{\lambda_c f}{\pi d_{\mathrm{in}}} 2\ln(2) \quad \text{(A9)}$$

we obtain the spatial wavelength content across the focal point

$$\Delta\lambda_{\mathrm{foc}} = \frac{\lambda_c g}{\pi d_{\mathrm{in}}} 2\ln(2)\sqrt{1-\left(\frac{\lambda_c}{2g}\right)^2} \quad \text{(A10)}$$

where d_{in} denotes the input diameter at FWHM of intensity. By aid of (A10) and (A8) the pulse duration in the focal point of the FP can be expressed as

$$\Delta t_{\mathrm{foc}} = \frac{\lambda_c d_{\mathrm{in}}}{gc}\left[1-\left(\frac{\lambda_c}{2g}\right)^2\right]^{-1/2}. \quad \text{(A11)}$$

REFERENCES

[1] M. Hentschel *et al.*, "Attosecond metrology," *Nature*, vol. 414, no. 6863, pp. 509–513, Nov. 2001.

[2] P. M. Paul *et al.*, "Observation of a train of attosecond pulses from high harmonic generation," *Science*, vol. 292, no. 5522, pp. 1689–1692, Jun. 2001.

[3] M. Y. Ivanov, R. Kienberger, a Scrinzi, and D. M. Villeneuve, "Attosecond physics," *J. Phys. B At. Mol. Opt. Phys.*, vol. 39, no. 1, pp. R1–R37, Jan. 2006.

[4] L. Chipperfield, J. Robinson, J. Tisch, and J. Marangos, "Ideal waveform to generate the maximum possible electron recollision energy for any given oscillation period," *Phys. Rev. Lett.*, vol. 102, no. 6, p. 063003, Feb. 2009.

[5] A. Wirth *et al.*, "Synthesized light transients," *Science*, vol. 334, no. 6053, pp. 195–200, Oct. 2011.

[6] S.-W. Huang *et al.*, "High-energy pulse synthesis with sub-cycle waveform control for strong-field physics," *Nature Photon.*, vol. 5, no. 8, pp. 475–479, Jul. 2011.

[7] C. Manzoni *et al.*, "Coherent synthesis of ultra-broadband optical parametric amplifiers," *Opt. Lett.*, vol. 37, no. 11, pp. 1880–1882, Jun. 2012.

[8] B. E. Schmidt *et al.*, "Frequency domain optical parametric amplification," *Nature Commun.*, vol. 5, art. no. 3643 (10 pages), may 2015.

[9] S. Witte, R. Th. Zinkstok, A. L. Wolf, W. Hogervorst, W. Ubachs, and K. S. E. Eikema, "A source of 2 terawatt, 2.7 cycle laser pulses based on noncollinear optical parametric chirped pulse amplification," *Opt. Express*, vol. 14, no. 18, pp. 8168–8177, 2006.

[10] A. Dubietis, R. Butkus, and a. P. Piskarskas, "Trends in chirped pulse optical parametric amplification," *IEEE J. Sel. Topics Quantum Electron.*, vol. 12, no. 2, pp. 163–172, Mar. 2006.

[11] H. Fattahi *et al.*, "Third-generation femtosecond technology," *Optica*, vol. 1, no. 1, pp. 45–64, Jul. 2014.

[12] C. Froehly, "Optical processing of picosecond laser pulses," *J. Opt.*, vol. 12, no. 1, pp. 25–34, Jan. 1981.

[13] E. Matsubara, K. Yamane, T. Sekikawa, and M. Yamashita, "Generation of 2.6 fs optical pulses using induced-phase modulation in a gas-filled hollow fiber," *J. Opt. Soc. Am. B*, vol. 24, no. 4, pp. 985–989, 2007.

[14] A. Baltuška and T. Kobayashi, "Adaptive shaping of two-cycle visible pulses using a flexible mirror," *Appl. Phys. B Lasers Opt.*, vol. 75, nos. 4/5, pp. 427–443, Oct. 2002.

[15] G. M. Gale, M. Cavallari, T. J. Driscoll, and F. Hache, "Sub-20-fs tunable pulses in the visible from an 82-MHz optical parametric oscillator," *Opt. Lett.*, vol. 20, no. 14, pp. 1562–1564, Jul. 1995.

[16] T. Wilhelm, J. Piel, and E. Riedle, "Sub-20-fs pulses tunable across the visible from a blue-pumped single-pass noncollinear parametric converter," *Opt. Lett.*, vol. 22, no. 19, pp. 1494–1496, Oct. 1997.

[17] T. Kobayashi and A. Shirakawa, "Invited paper Tunable visible and near-infrared pulse generator in a 5 fs regime," vol. 246, pp. 239–246, 2000.

[18] J. Rothhardt, S. Demmler, S. Hädrich, J. Limpert, and A. Tünnermann, "Octave-spanning OPCPA system delivering CEP-stable few-cycle pulses and 22 W of average power at 1 MHz repetition rate," *Opt. Exp.*, vol. 20, no. 10, pp. 10870–10878, May 2012.

[19] N. Ishii *et al.*, "Sub-two-cycle, carrier-envelope phase-stable, intense optical pulses at 1.6 μm from a BiB3O6 optical parametric chirped-pulse amplifier," *Opt. Lett.*, vol. 37, no. 20, pp. 4182–4184, Oct. 2012.

[20] J. Moses and S.-W. Huang, "Conformal profile theory for performance scaling of ultrabroadband optical parametric chirped pulse amplification," *J. Opt. Soc. Am. B*, vol. 28, no. 4, pp. 812–831, Mar. 2011.

[21] S. Ališauskas *et al.*, "Prospects for increasing average power of optical parametric chirped pulse amplifiers via multi-beam pumping," *Opt. Commun.*, vol. 283, no. 3, pp. 469–473, Feb. 2010.

[22] A. Harth *et al.*, "Two-color pumped OPCPA system emitting spectra spanning 1.5 octaves from VIS to NIR," *Opt. Exp.*, vol. 20, no. 3, pp. 3076–3081, Jan. 2012.

[23] T. Kobayashi, J. Liu, and K. Okamura, "Applications of parametric processes to high-quality multicolour ultrashort pulses, pulse cleaning and CEP stable sub-3fs pulse," *J. Phys. B At. Mol. Opt. Phys.*, vol. 45, no. 7, art. no. 074005 (17 pages), Apr. 2012.

[24] D. Herrmann *et al.*, "Approaching the full octave: Noncollinear optical parametric chirped pulse amplification with two-color pumping," *Opt. Exp.*, vol. 18, no. 18, pp. 18752–18762, Aug. 2010.

[25] G. Cerullo and S. De Silvestri, "Ultrafast optical parametric amplifiers," *Rev. Sci. Instrum.*, vol. 74, no. 1, pp. 1–18, 2003.

[26] I. Powell, "Design of a laser beam line expander," *Appl. Opt.*, vol. 26, no. 17, pp. 3705–3709, 1987.

[27] B. E. Schmidt *et al.*, "High harmonic generation with long-wavelength few-cycle laser pulses," *J. Phys. B At. Mol. Opt. Phys.*, vol. 45, no. 7, art. no. 074008 (9 pages), Apr. 2012.

[28] R. Trebino *et al.*, "Review article measuring ultrashort laser pulses in the time-frequency domain using frequency-resolved optical gating," vol. 68, no. 9, pp. 3277–3295, 1997.

[29] M. Kakehata *et al.*, "Single-shot measurement of carrier-envelope phase changes by spectral interferometry," *Opt. Lett.*, vol. 26, no. 18, pp. 1436–1438, Sep. 2001.

[30] A. Baltuška, T. Fuji, and T. Kobayashi, "Controlling the carrier-envelope phase of ultrashort light pulses with optical parametric amplifiers," *Phys. Rev. Lett.*, vol. 88, no. 13, p. 133901, Mar. 2002.

[31] H. Wang *et al.*, "Coupling between energy and phase in hollow-core fiber based f-to-2f interferometers," *Opt. Exp.*, vol. 17, no. 14, pp. 12082–12089, Jul. 2009.

[32] B. M. Hegelich *et al.*, "Laser acceleration of quasi-monoenergetic MeV ion beams," *Nature*, vol. 439, no. 7075, pp. 441–444, Jan. 2006.
[33] H. Schwoerer *et al.*, "Laser-plasma acceleration of quasi-monoenergetic protons from microstructured targets," *Nature*, vol. 439, no. 7075, pp. 445–448, Jan. 2006.
[34] C. Thaury *et al.*, "Plasma mirrors for ultrahigh-intensity optics," *Nature Phys.*, vol. 3, no. 6, pp. 424–429, Apr. 2007.
[35] U. Teubner *et al.*, "Anomalies in high-order harmonic generation at relativistic intensities," *Phys. Rev. A*, vol. 67, no. 1, p. 013816, Jan. 2003.
[36] F. Tavella, A. Marcinkevičius, and F. Krausz, "Investigation of the superfluorescence and signal amplification in an ultrabroadband multiterawatt optical parametric chirped pulse amplifier system," *New J. Phys.*, vol. 8 12 pages, 2006.
[37] C. Manzoni, J. Moses, F. X. Kärtner, and G. Cerullo, "Excess quantum noise in optical parametric chirped-pulse amplification," *Opt. Exp.*, vol. 19, no. 9, pp. 8357–8366, 2011.
[38] S. Witte *et al.*, "A source of 2 terawatt, 2.7 cycle laser pulses based on noncollinear optical parametric chirped pulse amplification," *Opt. Exp.*, vol. 14, no. 18, pp. 8168–8177, 2006.
[39] F. Tavella *et al.*, "High-dynamic range pulse-contrast measurements of a broadband optical parametric chirped-pulse amplifier," *Appl. Phys. B*, vol. 81, no. 6, pp. 753–756, Sep. 2005.
[40] I. A. Begishev *et al.*, "Highly efficient parametric amplification of optical beams. I. Optimization of the profiles of interacting waves in parametric amplification," *Sov. J. Quantum Electron.*, vol. 20, no. 9, pp. 1100–1103, Sep. 1990.

Philippe Lassonde received the Diploma degree in engineering physics from Université Laval, Québec City, QC, Canada, in 2006, and the M.Sc. degree in physics from Institut National de la Recherche Scientifique, Québec City, in 2009. He is currently working as a Research Professional at the Advanced Laser Light Source, Varennes, QC. His main research interests include ultrafast laser physics and technology.

Nicolas Thiré received the B.Sc. degree in physics and chemistry and the M.Sc. degree in physics from the University of Rennes I, Rennes, France, in 2006 and 2008, respectively. He received the Ph.D. degree in molecular physics from the University Paul Sabatier, Toulouse, France, in 2011. Since 2012, he holds a Postdoctoral Fellowship Position in Prof. Légaré's Group at the Institut National de la Recherche Scientifique, Québec City, QC, Canada. His research domains include intense laser source development, especially in the IR range and up to soft X-rays using high-order harmonics generation process, high harmonics spectroscopy, and ultrafast dynamics in gases and solids.

Ladan Arissian received the Ph.D. degree in optical science and engineering from the University of New Mexico, Albuquerque, NM, USA, in 2006. She joined the University of Texas A&M in 2008 as a Research Associate to work in the field of attosecond science at the National Research Council of Canada, Ottawa, ON, Canada. She has been with the University of New Mexico as a Faculty since 2010. She conducts experiments in nonlinear optics, laser-induced filamentation, and sensor developments based on frequency combs.

Guilmot Ernotte received the Diploma degree in engineering physics from École Polytechnique de Montréal, Montréal, QC, Canada, in 2014. He is currently working toward the M.Sc. degree in physics at the Institut National de la Recherche Scientifique, Québec City, QC. His research interests include femtosecond midinfrared lasers and nonlinear optics.

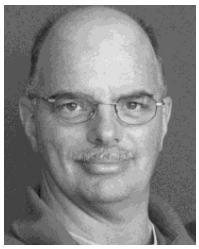

François Poitras received the Technical degree in technologie physique from Cégep de La Pocatière La Pocatière, QC, Canada, in 1978. He was a Laser Technician at the Institut National de la Recherche Scientifique-ÉMT from 1978 to 2013.

Tsuneyuki Ozaki received the Graduation, M.Sc., and Ph.D. degrees from the University of Tokyo, Tokyo, Japan, in 1987, 1989, and 1998, respectively. From 1990 to 2000, he was a Research Associate at the Institute for Solid State Physics, University of Tokyo. From 2000 to 2003, he was a Research Specialist at Nippon Telegraph and Telephone Basic Research Laboratories, Atsugi, Japan. In 2003, he joined the Institut National de la Recherche Scientifique as an Assistant Professor. He is currently a Full Professor, and the former Director of the ALLS facility. His main research interests include high-intensity terahertz radiation sources and their applications, intense high-order harmonic generation, and the use of lasers in medicine. He is currently serving on the Board of Directors of the International Committee on Ultrahigh Intensity Lasers.

Antoine Larameé received the Technical Diploma degree in physics from LaPocatière College, LaPocatière, QC, Canada, in 2003. He was with an industry developing and assembling laser diode source. Since 2008, he is working as a Research Technician at the Advanced Laser Light Source, Varennes, QC, operating, maintaining, and installing femtosecond and YAG laser source, as well as characterizing them.

Maxime Boivin received the B.Ing. degree from Université Laval, Quebec City, QC, Canada, in 2012.

Heide Ibrahim received the Ph.D. degree in coherent control schemes from Freie Universität Berlin, Berlin, Germany, in 2008. She continued in this field as a Postdoctoral Researcher at the Institute for Molecular Science, Okazaki, Japan, before she moved on to the Institut National de la Recherche Scientifique (INRS), Québec City, to work with dynamic transmission electron microscopy and ultrafast electron diffraction. She is currently a Research Associate at the INRS and interested in ultrafast imaging of molecular rearrangements by Coulomb explosion imaging and on laser source development based on Fourier-domain nonlinear optics.

François Légaré received the B.Sc., M.Sc., and Ph.D. degrees in chemistry from Université de Sherbrooke, Sherbrooke, QC, Canada, in 1998, 2001, and 2004, followed by postdoctoral studies at Harvard University, Cambridge, MA, USA, from 2004 to 2006. He joined the Institut National de la Recherche Scientifique-ÉMT in 2006 and became a full Professor in 2013. His research team is working on the development of few-cycle laser technologies for applications in AMO physics, and the applications of laser technology for biomedical imaging. He is the Director of the Laboratory for the Applications of Nonlinear Optical Microscopy in Biomedical Imaging and of the Advanced Laser Light Source.

Bruno E. Schmidt received the Dipl.Ing. degree in optical engineering from the University of Applied Science, Cologne, Germany, in 2003. In 2003, he was a Scientific Assistant at the University of Applied Science, Remagen, Germany, on building an XUV interferometer. He continued with the Physics Department at the Freie Universität Berlin, Berlin, Germany, where he received the Ph.D. degree in 2008 in coherent control and filamentation. From 2009 to 2013, he was a Postdoctoral Fellow in the Group of Prof. Légaré at the Institut National de la Recherche Scientifique where he continued as a Research Associate. His research interests include laser development and its application for high harmonic generation, in particular, he works on high energy few-cycle IR pulse compression and amplification. He developed the FOPA and founded few-cycle Inc. in late 2013 to commercialize FOPA and related technologies.